Medical Physics
The International Journal of Medical Physics Research and Practice

Optimization of a dual-energy contrast-enhanced technique for a photon-counting digital breast tomosynthesis system: II. An experimental validation

Ann-Katherine Carton, Christer Ullberg, and Andrew D. A. Maidment

Citation: Medical Physics **37**, 5908 (2010); doi: 10.1118/1.3488889
View online: http://dx.doi.org/10.1118/1.3488889
View Table of Contents: http://scitation.aip.org/content/aapm/journal/medphys/37/11?ver=pdfcov
Published by the American Association of Physicists in Medicine

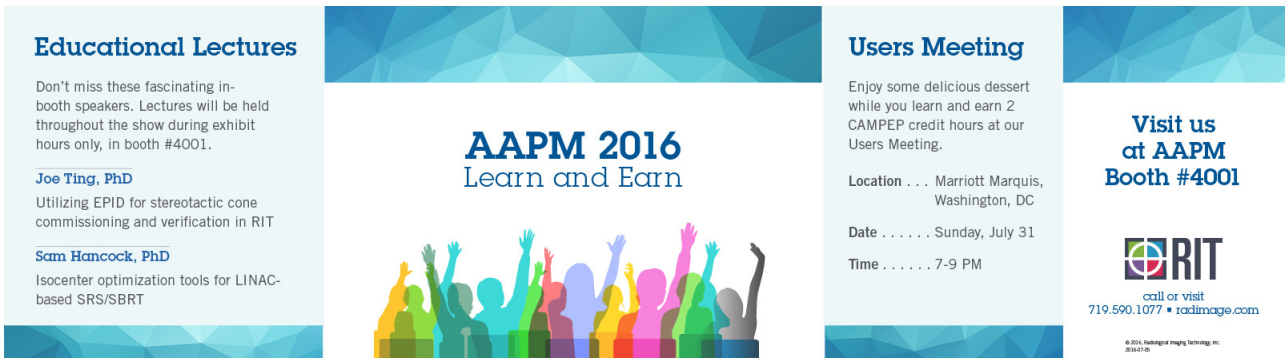

Optimization of a dual-energy contrast-enhanced technique for a photon-counting digital breast tomosynthesis system: II. An experimental validation

Ann-Katherine Carton
University of Pennsylvania, Philadelphia, Pennsylvania 19104

Christer Ullberg
XCounter AB, Svärdvägen 11, SE-182 33 Danderyd, Sweden

Andrew D. A. Maidment[a)]
University of Pennsylvania, Philadelphia, Pennsylvania 19104

(Received 22 August 2009; revised 22 August 2010; accepted for publication 23 August 2010; published 20 October 2010)

Purpose: Previously, the authors developed a dual-energy (DE) acquisition technique for a photon-counting digital breast tomosynthesis (DBT) imaging system. Low-energy (LE) and high-energy (HE) images are acquired in a single scan by covering alternate slits of a multislit prepatient collimator with Sn and Cu, respectively. A theoretical model was used to optimize the technique. In this article, an experimental validation of this technique is presented.

Methods: Experiments were performed on a prototype DBT system. LE and HE projection images were acquired sequentially; either a Sn or a Cu filter was positioned in the filter holder at the exit window of the x-ray tube. Sn filters from 0.113 to 0.242 mm thick and Cu filters from 0.103 to 0.267 mm were used. The images were acquired with a W target at 49 kV. Tomographic images, hereafter referred to as DBT images, were reconstructed using a shift-and-add algorithm. DE-DBT images were obtained by weighted logarithmic subtraction of the LE and HE images. Weighting factors w_t that optimally cancel breast tissues with two different glandularities were assessed for 20–80 mm thick phantoms with 0%, 50%, and 100% glandularity. The mean and standard deviation in the per-pixel signal intensity (SI) were calculated in the DBT images. These data were used to calculate signal-difference-to-noise ratios (SDNRs) between iodine enhanced and nonenhanced polymethyl methacrylate backgrounds. To illustrate the feasibility of the technique, DE-DBT images of a structured phantom containing iodine disks were assessed. The experimental results were compared against the values obtained from a theoretical model of the imaging system.

Results: The average difference between theoretical and experimental w_t was found to range from 8% to 21%. Experimental w_t values increase with phantom thickness and Cu thickness, depend somewhat on Sn thickness, and vary more as a function of breast composition in thick breasts than in thin breasts. Theoretical and experimental mean and standard deviation in the per-pixel SI differ by −7% to 10% and by −3% to 4%. Theoretical and experimental SDNR values differ, on average, by 1.5%. Iodine concentrations can be predicted from SDNR; the relationship can be accurately fit to a quadratic. In the images of the structured phantom, iodine concentrations of 1 $\mathrm{mg/cm^2}$ and larger are discernable.

Conclusions: The strong agreement between experimental and theoretical results in this article indicates that the authors' computer model is accurate. [DOI: 10.1118/1.3488889]

Key words: digital breast tomosynthesis, dual-energy, iodine contrast-enhanced imaging

I. INTRODUCTION

Contrast-enhanced (CE) digital breast tomosynthesis (DBT) is a novel modality for imaging breast lesion morphology and vascularity. Recent research, both experimental and theoretical, has shown that CE-DBT is feasible in clinical practice at radiation doses equivalent to conventional mammography.[1,2]

In dual-energy (DE) CE imaging, low-energy (LE) and high-energy (HE) images are acquired after an intravenous injection of an iodinated contrast agent. These images are then combined into iodine and soft tissue images.[2,3] Key technical parameters that determine the detectability of the iodine are the x-ray spectra used to produce the LE and HE images, the dose allocation between the LE and HE images, and the total dose to the patient.

In a companion paper,[4] we developed a DE acquisition technique for a photon-counting DBT imaging system. LE and HE images are acquired in a single scan by differentially filtering fan beams defined by a multislit prepatient collimator.[4] Sn and Cu filters are used to acquire LE and HE images at a tube voltage of 49 kV. A theoretical model was used to determine the optimal thickness of the Sn and Cu

TABLE I. Comparison of experimental and theoretical assessed HVLs, QVLs, EVLs, and TVLs of the W target, filtered with 0.185 mm Sn at 49 kV.

	HVL (mm Al)	QVL (mm Al)	EVL (mm Al)	TVL (mm Al)
Experimental	1.306	2.786	4.414	5.003
Theoretical	1.300	2.806	4.539	5.154

filters, dose allocation between the LE and HE images, and mean glandular dose. These optima were computed to maximize iodine detectability as characterized by the signal-difference-to-noise ratio (SDNR) in the DE-DBT images.

In this paper, an experimental validation of the DE acquisition technique is presented using a prototype DE-DBT system. Results from our theoretical model are compared to measured optimal weighting factors w_t for the logarithmic subtraction, mean and standard deviations in the signal intensity (SI), and SDNR in iodine enhanced phantom images.[4] In addition, DE-DBT images of a structured phantom containing iodine were assessed to illustrate the feasibility of the technique.

II. MATERIAL AND METHODS

II.A. Imaging system

Experimental measurements were performed on a prototype XC Mammo-3T DBT system (XCounter, Danderyd, Sweden). A detailed description of this system has been presented previously.[5,6] The system was modified to allow DE CE imaging. As previously described,[4] we propose a system design where LE and HE images are acquired in a single scan in which alternate slits of the multislit prepatient collimator are covered with Sn and Cu. Note, however, that the experiments described in this paper were performed by acquiring LE and HE images sequentially; either a Sn or a Cu filter was positioned in the filter holder at the exit window of the x-ray tube. The choice of the filter thicknesses was guided by our previous theoretical analysis.[4] Sn filters of 0.113, 0.170, 0.185, and 0.242 mm, and Cu filters of 0.103, 0.164, 0.206, and 0.267 mm were used (Alfa Aesar, Ward Hill, MA). The thickness of the filters was measured with a micrometer.

The experiments were performed at an x-ray tube voltage of 49 kV. Table I shows the measured half value layer (HVL), quarter value layer (QVL), eighth value layer (EVL), and tenth value layer (TVL) of the W target, filtered with 0.185 mm Sn.

Projection mages were acquired at 70 mA, half the maximum feasible tube loading, with a scan time of 10 s using the detector at full resolution (60×60 μm^2/pixel). The projection images were processed to correct for gain and a 2×2 software binning was applied prior to reconstruction. Tomographic images (hereafter referred to as *DBT images*) were reconstructed using a shift-and-add algorithm. The DBT images were reconstructed from the full set of 48 projection images. The DBT images were reconstructed in 1 mm increments with an in-plane pixel size of 120×120 μm^2.

Note that the 1:1 fixed system configuration proposed in the companion paper[4] using 49 kV and 140 mA is simulated; twice the number of projection images are acquired within a single scan, each at half the mA.

II.B. Weighting factors

Iodine enhanced DBT images (hereafter referred to as *DE-DBT images*) were obtained by weighted logarithmic pixel-by-pixel subtraction of the HE-DBT and the LE-DBT images. The SI in the DE-DBT images, SI_{DE}, can be written as

$$SI_{DE} = \ln[SI_{Cu}] - w_t \cdot \ln[SI_{Sn}], \tag{1}$$

where SI_{Cu} and SI_{Sn} refer to the HE-DBT images filtered with Cu and the LE-DBT images filtered with Sn, respectively. The weighting factor w_t was optimized to cancel the subject contrast between two breast equivalent materials with different glandularity. Optimal w_t values were evaluated using 0%, 50%, and 100% glandular tissue equivalent phantoms with 20, 40, 60, and 80 mm thickness (CIRS, Norfolk, VA). The phantoms were scanned with the above Sn and Cu filters. DE-DBT images were obtained by varying w_t from 0 to 1 in steps of 0.01.

The subject contrast C between two different breast equivalent materials in the DE-DBT images was computed as

$$C = \frac{\overline{SI}_{DE_{f_{g1}}} - \overline{SI}_{DE_{f_{g2}}}}{1/2 \cdot (\overline{SI}_{DE_{f_{g1}}} + \overline{SI}_{DE_{f_{g2}}})}, \tag{2}$$

where $\overline{SI}_{DE_{f_{g1}}}$ and $\overline{SI}_{DE_{f_{g2}}}$ are the means in the per-pixel SI in breast equivalent materials with glandular equivalents f_{g1} and f_{g2}. $\overline{SI}_{DE_{f_{g1}}}$ and $\overline{SI}_{DE_{f_{g2}}}$ were computed in 1 cm diameter circular regions of interest (ROIs). The optimal w_t was defined as that which minimizes C. This is equivalent to the previously derived theoretical calculation of w_t.[4] The mean and standard deviation in w_t were computed from five repeated scans for each of the 192 experimental conditions (16 Sn–Cu filter pairs $\times$ 3 glandular equivalent combinations $\times$ 4 phantom thicknesses).

II.C. Signal-difference-to-noise ratio

SDNR per pixel was calculated as a measure of the detectability of iodine in the DE-DBT images. SDNR was defined as

$$SDNR = \frac{\overline{SI}_{DE_B} - \overline{SI}_{DE_I}}{\sigma^{DBT}_{DE_B}}, \tag{3}$$

where $\overline{SI}_{DE_B}$ and $\overline{SI}_{DE_I}$ are the mean per-pixel SI in a background region B and iodine enhanced region I in the DE-DBT image, and σ_{DE_B} is the standard deviation in SI_{DE_B}. SDNR was evaluated using polymethyl methacrylate (PMMA) as a phantom material instead of breast tissue equivalent materials used in the previous experiment. We

were required to use a PMMA phantom, since it was the only phantom available to us containing iodine disks of known concentration. A 27 mm thick homogenous PMMA phantom containing iodine disks with areal concentrations of 0.5, 1, 2, 4, 10, and 20 mg I/cm^2 (Nuclear Associates, Johnson City, TN) was scanned alone or together with a 20 mm homogeneous PMMA slab. The scans were performed with all of the above listed Sn and Cu filters. DE-DBT images were obtained using w_t values that optimally cancel the subject contrast between 0% and 50% glandular tissue equivalents. $\overline{\mathrm{SI}}_{\mathrm{DE}_I}$ values were measured in 1 cm diameter circular ROI of the iodine disks; $\overline{\mathrm{SI}}_{\mathrm{DE}_B}$ and σ_{DE_B} were measured in a neighboring 1 cm diameter circular ROI of PMMA only. All measurements were performed in the DE-DBT image in which the iodine disks were in focus. In addition, the relationship between SDNR and the corresponding iodine areal concentration was assessed.

II.D. Structured phantom

An experiment was also performed to evaluate the conspicuity of iodine in DE-DBT images using a structured phantom. The phantom consists of two parts. The first consists of a 3.5 cm thick PMMA box filled with 1/2, 1/4, and 3/8 in. diameter PMMA spheres and mineral oil. The spheres were homogenously distributed in the box. This part provides a structured background. The second part of the phantom consists of the 27 mm thick homogenous PMMA slab in which iodine disks of known areal concentrations are embedded as described in Sec. II C. The two parts were stacked such that the iodine disks were in contact with the structured portion. The phantom was scanned with the 0.185 mm Sn and 0.205 mm Cu filter at 49 kV and 70 mA. DE-DBT images were obtained using a w_t value that minimizes the relative standard deviation in the per-pixel SI of the structured background. The conspicuity of iodine was evaluated in the DE-DBT image that had the iodine disks in focus.

II.E. Theoretical model

The experiments described in Secs. II C and II D were simulated using a theoretical model of the XC Mammo-3T DBT system. Details of the theoretical model were described previously.[4] The simulation was performed using the same x-ray spectra, system configuration, x-ray exposures, and phantoms as those of the experiments described here.

X-ray spectra were simulated using a validated extrapolation of Boone's low-energy mammographic x-ray spectra.[7,8] We validated our simulated spectra using least-square comparison (χ^2 values) between attenuation data from our simulated spectra and attenuation data measured on the XC Mammo-3T system. Attenuation curves were obtained by filtering the spectra with Al. The χ^2 was minimized by adding 0.251 mm Al to the simulated spectra. Table I summarizes the attenuation curves by comparing theoretically and experimentally assessed HVL, QVL, EVL, and TVL for a W target spectrum filtered with 0.185 mm Al at 49 kV; 0.251 mm Al was added to the simulated spectra.

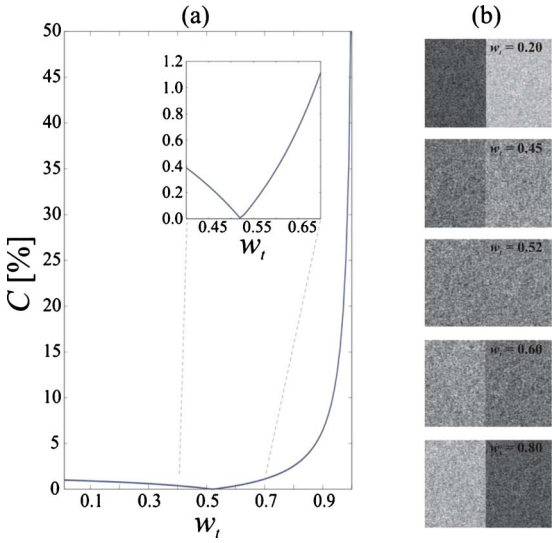

FIG. 1. (a) C between 0% and 50% glandular breast equivalents as a function of w_t for a 0.185 mm Sn–0.267 mm Cu combination in a 20 mm thick phantom. (b) ROI including both of the glandular tissue equivalents for a selected set of w_t. The same window/level was applied for all images.

PMMA was modeled using elemental composition and mass density provided by NIST;[9] breast tissue equivalent materials were modeled using elemental compositions and mass densities provided by CIRS. In the results below, the experimental and theoretical results are compared.

III. RESULTS

III.A. Weighting factors

C was calculated for all parameter combinations (16 Sn–Cu filter pairs $\times$ 3 glandular equivalent combinations $\times$ 4 phantom thicknesses). Figure 1(a) illustrates C as a function of w_t for a 0.185 mm Sn–0.267 mm Cu filter pair, with a 0%–50% glandular equivalent combination and a 20 mm phantom. Figure 1(b) shows a ROI including both of the glandular equivalents for a selected set of w_t. The same window and level values were applied in all images. These images clearly show that the subject contrast between the two glandularities is completely canceled when the optimal $w_t = 0.52$ is applied.

Figures 2(a) and 2(b) compare theoretical and experimental w_t values that optimally cancel the subject contrast between 0% and 100% glandular equivalents in DE-DBT images of 20, 40, 60, and 80 mm thick phantoms. Figure 2(a) shows optimal w_t values for a 0.170 mm Sn filter with 0.103–0.267 mm thick Cu filters. This figure shows that theoretical and experimental w_t decrease with increasing Cu thickness. This trend is similar for the other three Sn filters. Figure 2(b) shows optimal w_t values for a 0.206 mm Cu filter combined with 0.113–0.242 mm thick Sn filters. This figure shows that for a 60 mm thick phantom, the optimal theoretical w_t values are almost independent of Sn thickness, while for 20, 40, and 80 mm thick phantoms the magnitude of the optimal theoretical w_t values varies somewhat with Sn thickness. This trend is similar for the other three Cu filters. Note

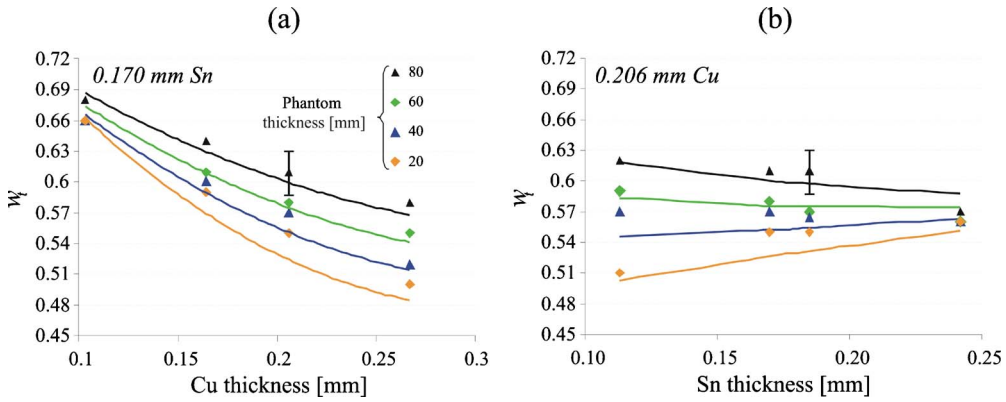

FIG. 2. Comparison of theoretical and experimental w_t values that optimally cancel 0% and 100% glandular tissue compositions in DE-DBT images of 20, 40, 60, and 80 mm thick phantoms. (a) Optimal w_t values as a function of Cu filter thickness for a 0.17 mm Sn filter thickness. (b) Optimal w_t values as a function of Sn filter thickness for a 0.206 mm Cu filter. Triangles represent experimental w_t values; lines represent theoretical w_t values. The error bars show typical standard deviations in the mean on experimental values of w_t; the standard deviations were computed from five repeated scans for each experimental condition.

that these trends are within one standard deviation in w_t; standard deviations were computed from the five repeated scans for each of the experimental conditions.

Figure 3 compares theoretical and experimental w_t values that optimally cancel the subject contrast between 0% and 50%, 0% and 100%, and 50% and 100% glandular tissue equivalents in DE-DBT images of 20, 40, 60, and 80 mm thick phantoms. Optimal w_t values are shown for a 0.170 mm Sn and 0.206 mm Cu filter combination. Figure 3 shows that w_t varies more as a function of breast tissue composition in thick breasts than in thin breasts. Optimal w_t increases when the percent by volume of glandular tissue increases. These observations are similar for the other Sn–Cu filter combinations. For a given filter pair, optimal theoretical, and experimental w_t values are larger for thick phantoms [Figs. 2(a), 2(b), and 3].

The difference between theoretical and experimental optimal w_t was found to range from −8% to 21% for the parameter combinations tested (16 Sn-Cu filter pairs × 3 glandular equivalent combinations × 4 phantom thicknesses).

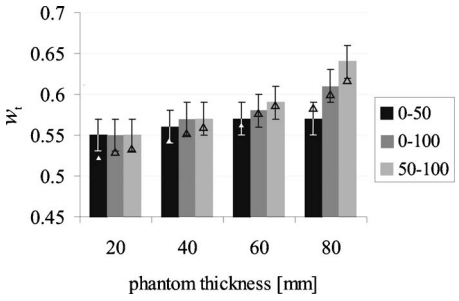

FIG. 3. Comparison of theoretical and experimental w_t values that optimally cancel 0% and 50%, 0% and 100%, and 50% and 100% glandular tissue compositions in DE-DBT images of 20, 40, 60, and 80 mm thick phantoms. LE and HE images were acquired with a 0.170 mm Sn and a 0.206 mm Cu filter. Bars show experimental w_t values; triangles show theoretical w_t values. Error bars show standard deviations in the mean of experimental values. Optimal w_t varied more as a function of breast tissue composition in thick than in thin breasts.

III.B. Signal-difference-to-noise ratio

Theoretical and experimental values of $\overline{\mathrm{SI}}_{\mathrm{DE}_I}$, $\overline{\mathrm{SI}}_{\mathrm{DE}_B}$, σ_{DE_B}, and SDNR were computed for all 16 Sn–Cu filter combinations, two phantom thicknesses, and six areal iodine concentrations described in Sec. II. For all conditions, it was found that the theoretical and experimental values of $\overline{\mathrm{SI}}_{\mathrm{DE}_I}$ and $\overline{\mathrm{SI}}_{\mathrm{DE}_B}$ differ by −7% to 10%. Theoretical and experimental values of σ_{DE_B} differ by −3% to 4%. The average difference between theoretical and experimental SDNR values was found to be 1.5% for the parameter conditions tested (16 Sn–Cu filter pairs × 2 phantom thicknesses × 6 areal iodine concentrations).

Figure 4 compares theoretical and experimental SDNR values as a function of areal iodine concentration in a DE-DBT image of the 57 mm thick PMMA phantom. A 0.185 mm Sn and a 0.206 mm Cu filter were used to obtain the LE and HE images. It was found that a linear fit to the theoretical SDNR values results in an absolute error of less than 0.08 for small iodine concentrations, but that a quadratic equation results in an absolute error of less than 0.001. Simi-

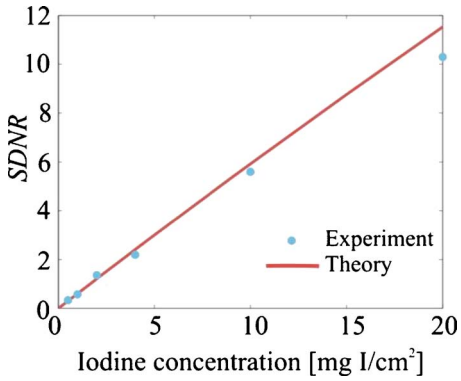

FIG. 4. Experimental and theoretical SDNR as a function of iodine concentration. These results are shown for a 57 mm thick phantom that was scanned at 49 kV with 70 mA. A 0.185 mm Sn and a 0.206 mm Cu filter were used to obtain the LE and HE images.

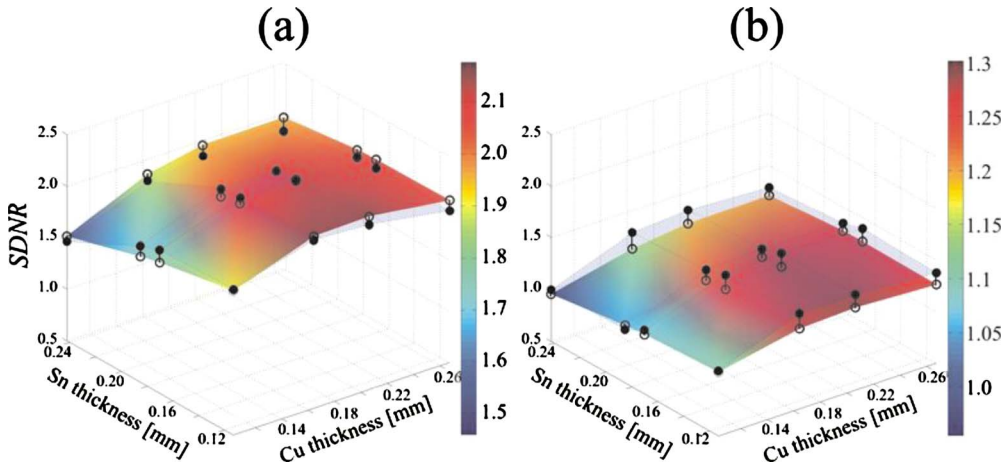

FIG. 5. Theoretical and experimental SDNR values in DE-DBT images from all studied Sn–Cu filter combinations. Sn and Cu images of the (a) 27 and (b) 57 mm thick phantoms were acquired at 70 mA. The SDNR values were computed for iodine disks with 2 mg I/cm^2. Solid spheres are experimental SDNR values; hollow spheres are theoretical SDNR values. The colored surfaces show the variation of the theoretical SDNR for intermediate Sn and Cu thicknesses.

lar results were found for all Sn–Cu filter pairs. These results suggest that SDNR values in subtraction images can be used to estimate the iodine area density when the appropriate quadratic transformation is known.

Figure 5 shows theoretical and experimental SDNR values for 2 mg I/cm^2 for all 16 studied Sn–Cu filter combinations and the two phantom thicknesses. For both phantom thicknesses, the experimental and theoretical SDNR values are maximal for the 0.113 mm Sn–0.206 mm Cu filter combination.

III.C. Structured phantom

Figure 6 illustrates a LE, HE, and DE-DBT image of the structured phantom. The LE and HE images were acquired with 0.185 mm Sn and 0.205 mm Cu filters. The 4, 2, and 1 mg $/cm^2$ iodine disks are in the field of view. DE-DBT images were obtained using a w_t value of 0.53. This value was found to cancel the structured background optimally. The images depict the iodine disks in focus. Iodine concentrations of 1 mg $/cm^2$ are discernable.

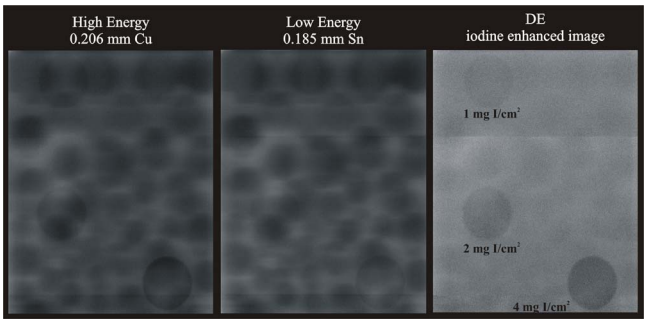

FIG. 6. Cu, Sn, and iodine DE-DBT images of a 57 mm thick structured phantom. The 0.185 mm Sn and 0.205 mm Cu images were acquired at 70 mA.

IV. DISCUSSION AND CONCLUSION

Previously, we proposed a DE contrast-enhanced technique for the photon-counting XC Mammo-3T system whereby LE and HE images are acquired in a single scan.[4] To optimize the DE technique, a theoretical model was used. This paper presents an experimental validation of this theoretical model.

We have shown that the differences between experimental and theoretical optimal w_t values are within experimental error. Experimental and theoretical $\overline{\mathrm{SI}}_{\mathrm{DE}_I}$, $\overline{\mathrm{SI}}_{\mathrm{DE}_B}$, and σ_{DE_B} show very good agreement. We have shown that we are able to simulate trends in SDNR as a function of the Sn–Cu filter pair and phantom thickness in close agreement with experimentally assessed values. It is worth noting that the maximum experimental SDNR occurs at 0.113 mm Sn and 0.206 mm Cu. This is consistent with the theoretical calculation.

The images in Fig. 6, which demonstrates the detectability of iodine in a structured phantom background, illustrate the feasibility of the technique. However, additional studies investigating the detectability of iodine in more realistic backgrounds are necessary because the material properties and frequency content of the structured phantom do not exactly match those of real breasts. In our ongoing work, a more realistic breast phantom based on the breast model by Bakic *et al.*[10] is used.

Identification of the optimal image acquisition technique is an important step in the implementation of new imaging technologies. In an accompanying paper, a theoretical model was used to optimize the technique for DE CE-DBT with the XC Mammo-3T system. The good match between experimental and theoretical values in this work indicates that the optima based on our computer model are accurate.

ACKNOWLEDGMENTS

The authors acknowledge the financial support of XCounter, Philips Medical Systems/RSNA Research Seed Grant 2005, the Department of Defense Concept Award No.

W81XWH-06-1-0613, and the National Cancer Institute Grant No. PO1-CA85484.

[a]Author to whom correspondence should be addressed. Electronic mail: Andrew.Maidment@uphs.upenn.edu; Telephone: +1-215-746-8763; Fax: +1-215-746-8764.

[1]S. Puong, X. Bouchevreau, F. Patoureaux, R. Iordache, and S. Muller, "Dual-energy contrast enhanced digital mammography using a new approach for breast tissue canceling," in *Proceedings of the Medical Imaging 2007 Conference: Physics of Medical Imaging*, Vol. 6510, edited by J. Hsieh and M. J. Flynn (SPIE, San Diego, 2007).

[2]S. Puong, F. Patoureaux, R. Iordache, and S. Muller, "Dual-energy contrast enhanced digital breast tomosynthesis: concept, method, and evaluation on phantoms," in *Proceedings of the Medical Imaging 2007 Conference: Physics of Medical Imaging*, Vol. 6510, edited by J. Hsieh and M. J. Flynn (SPIE, San Diego, 2007).

[3]A.-K. Carton, K. Lindman, C. K. Ullberg, and T. Francke, "Dual-energy subtraction for contrast enhanced digital breast tomosynthesis," in *Proceedings of the Medical Imaging 2007 Conference: Physics of Medical Imaging*, Vol. 6510, edited by J. Hsieh and M. J. Flynn (SPIE, San Diego, 2007).

[4]A.-K. Carton, C. Ullberg, K. Lindman, R. Acciavatti, T. Francke, and A. D. A. Maidment, "Optimization of a dual-energy contrast-enhanced technique for a photon counting digital breast tomosynthesis system: I. A theoretical model," Med. Phys. **37**, 5896–5907 (2010).

[5]A. D. A. Maidment *et al.*, "Evaluation of a photon-counting breast tomosynthesis imaging system," in *Proceedings of the Medical Imaging 2005 Conference: Physics of Medical Imaging*, Vol. 5745, edited by M. J. Flynn (SPIE, San Diego, 2005).

[6]A. D. A. Maidment *et al.*, "Evaluation of a photon-counting breast tomosynthesis imaging system," in *Proceedings of the Medical Imaging 2006 Conference: Physics of Medical Imaging*, Vol. 6142, edited by M. J. Flynn and J. Hsieh and M. J. Flynn (SPIE, San Diego, 2006).

[7]J. M. Boone, T. R. Fewell, and R. J. Jennings, "Molybdenum, rhodium, and tungsten anode spectral models using interpolating polynomials with application to mammography," Med. Phys. **24**, 1863–1874 (1997).

[8]A.-K. Carton, J. Li, S. C. Chen, E. F. Conant, and A. D. A. Maidment, "Optimization of contrast-enhanced digital breast tomosynthesis," Lect. Notes Comput. Sci. **4046**, 183–189 (2006).

[9]http://physics.nist.gov/PhysRefData/XrayMassCoef/cover.html. Last accessed May 2009.

[10]A. K. Carton, P. Bakic, C. Ullberg, H. Derand, and A. D. A. Maidment, "Development of a 3D physical anthropomorphic breast phantom," in Proceedings of the Tomosynthesis Imaging Symposium 2009: Frontiers in Research and Clinical Applications, Duke University, 2009.